Composite Aerogels

DOI: 10.1002/ange.201105730

Cellulose–Silica Nanocomposite Aerogels by In Situ Formation of Silica in Cellulose Gel**

Jie Cai, Shilin Liu, Jiao Feng, Satoshi Kimura, Masahisa Wada, Shigenori Kuga,* and Lina Zhang*

Aerogels with their low density (0.004–0.500 $g\,cm^{-3}$), large internal surface area, and large open pores are promising candidates for various advanced applications.[1] The utilization of inorganic aerogels, however, has been hampered by their poor mechanical properties. A prominent example is silica aerogel, which is prepared by an organic sol–gel process,[2] and has unique features, such as ultralow density (the lightest silica aerogel has a density that is similar to the density of air, which is 0.00129 $g\,cm^{-3}$), near transparency, and low thermal conductivity. However, the extreme fragility of this aerogel necessitates its reinforcement for practical uses. A typical method is hybridization with organic polymers, such as polyurea, polyurethane, poly(methyl methacrylate), polyacrylonitrile, and polystyrene.[3]

Other candidates for the reinforcement of inorganic aerogels are insoluble polysaccharides, which are abundantly available and show wide varieties in structure and properties.[4] The useful features of these compounds are hydrophilicity, biocompatibility, hydroxy reactivity, and reasonable thermal and mechanical stabilities.[5] For example, nanofibrillar bacterial cellulose and microfibrillated cellulose gel have been proposed as templates for cobalt ferrite nanoparticles and titanium dioxide.[6]

While in the above-mentioned work native cellulose with cellulose I crystallinity was used, cellulose can be prepared as a hydrogel with cellulose II crystallinity through dissolution and coagulation. Some of the resulting aerogels have remarkable mechanical strength and light transmittance.[7] They have high porosity with open structures and thus provide an effective substrate for the synthesis of metallic nanoparticles.[8] To further utilize the regenerated cellulose gel, we herein attempted in situ synthesis of silica in cellulose gels. While a similar attempt has been reported, in which the cellulose gel was obtained from solution in *N*-methylmorpholine-*N*-oxide monohydrate,[9] the development of the nanostructure (nitrogen BET surface area of 220–290 $m^2\,g^{-1}$) and the level of silica loading (less than 13% *w*/*w*) were rather limited. By using the aqueous alkali-based solvent, we obtained the cellulose aerogel with a surface area of 356 $m^2\,g^{-1}$, and a silica loading of more than 60% *w*/*w* resulted in surface areas that exceeded 600 $m^2\,g^{-1}$.

We used the sol–gel synthesis method toward nanostructured silica, which typically starts from tetraethyl orthosilicate (TEOS). The resulting composite gels were dried with supercritical CO_2 to give cellulose–silica aerogels with low density, moderate light transmittance, a large surface area, high mechanical integrity, and excellent heat insulation. This method can also lead to fabrication of silica-only aerogels through the removal of cellulose by calcination, that is, the use of cellulose aerogel as sacrificial template.

Figure 1 shows the preparation of the aerogel. The cellulose hydrogel is a transparent material that has a water content of 92% and a porosity of 95%. The sol–gel process catalyzed by ammonia converts TEOS to SiO_2, which is deposited on the cellulose network (Figure 1b). The composite is converted to an aerogel by drying with supercritical CO_2 to maintain the porous structure (Figure 1c), thus resulting in a flexible and translucent cellulose–silica aerogel. Subsequent calcination removes the cellulose matrix to give a silica-only aerogel (Figure 1d and g).

The cellulose aerogel is composed of regenerated cellulose fibrils, which are typically less than 10 nm wide (Figure 2a). The BET surface area of 356 $m^2\,g^{-1}$ (determined by

[*] Dr. J. Cai, J. Feng, Prof. L. Zhang
College of Chemistry and Molecular Sciences
Wuhan University, Wuhan, 430072 (China)
E-mail: jiecaiwhu@hotmail.com
Homepage: http://www.polyphys.whu.edu.cn/
Dr. J. Cai, S. Liu, S. Kimura, M. Wada, Prof. Dr. S. Kuga
Graduate School of Agricultural and Life Sciences
The University of Tokyo (Japan)
E-mail: askuga@mail.ecc.u-tokyo.ac.jp

[**] This work was supported by the Japan Society for the Promotion of Science (JSPS) Foreign Researcher Fund of Japan, the National Basic Research Program of China (973 Program, 2010CB732203), the National Natural Science Foundation of China (20904043), and the Foundation of Key Laboratory of Cellulose and Lignocellulosic Chemistry, Chinese Academy of Sciences, China.

Supporting information for this article is available on the WWW under http://dx.doi.org/10.1002/anie.201105730.

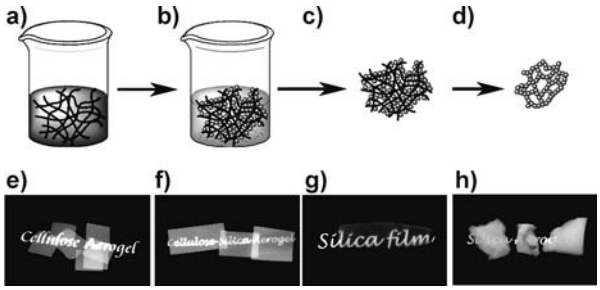

Figure 1. Top: Aerogel preparation. a) Nanoporous cellulose gel with interconnected nanofibrillar network is impregnated with silica precursor TEOS (in $MeOH/H_2O$). b) Silica formation by hydrolysis and condensation (sol–gel process with $NH_3{\cdot}H_2O$), giving cellulose–silica composite gel. Drying with supercritical CO_2 gives c) composite aerogel. Calcination of cellulose leaves d) mesoporous silica aerogel. Bottom: Macroscopic views of e) C0, f) C2, g) C2-S, and h) S0.

nitrogen adsorption, Table 1) translates to a fibril width of 7 nm, thus agreeing well with the SEM image. The cellulose aerogel, which is approximately 0.35 mm thick (Figure 1e), was fairly transparent, thus demonstrating its homogeneous nanoporosity. The composite aerogel C2 shows apparent deposition of silica nanoparticles onto the cellulose network (Figure 2b). The surface area of C2 is 474 $m^2 g^{-1}$ and is thus between those of samples C0 and S0, as expected. Also remarkable is the moderate transparency of the composite aerogels (Figure 1f), which indicates a homogeneous dispersion of silica in the aerogel.

The cellulose-templated silica has a fibrillar morphology, while the pure silica aerogel seems to form an isotropic network (Figure 2c and d, respectively). These features are more clearly shown in TEM images of ultrathin sections (Figure 3). The composite (Figure 3b) seems to be a superposition of a pure cellulose network (Figure 3a) and pure silica gel (Figure 3d), but the cellulose-templated silica obtained by calcination of the composite (Figure 3c) has a fabrillar morphology that is inherited from the cellulose network.

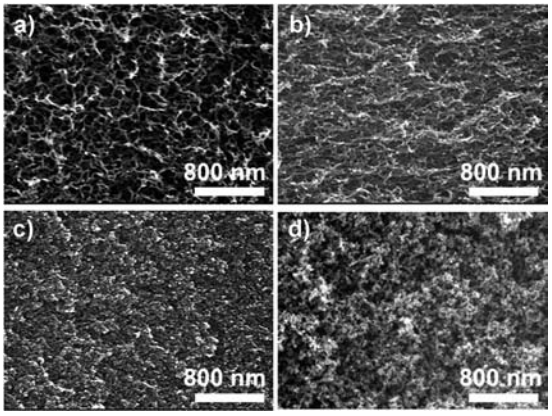

Figure 2. Scanning electron microscopy (SEM) images of a) C0, b) C2, c) C2-S, and d) S0.

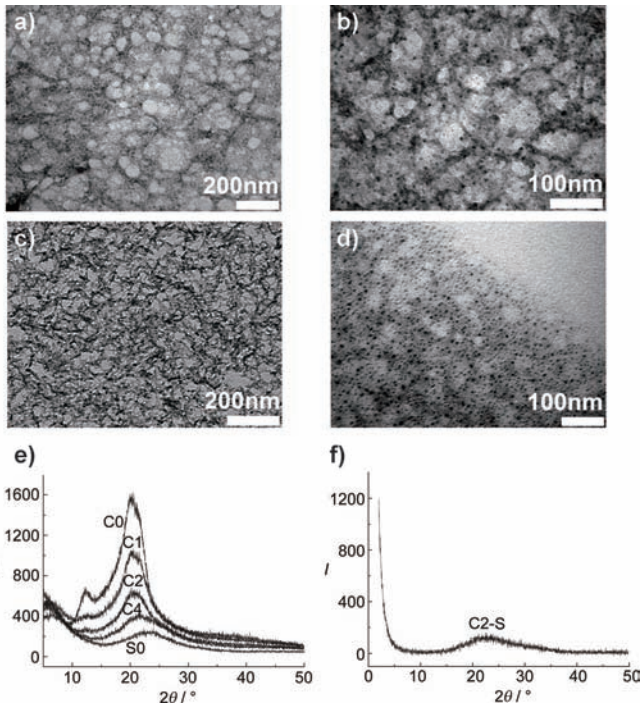

Figure 3. Transmission electron microscopy (TEM) images of a) C0, b) C2, c) C2-S, and d) S0. Wide-angle X-ray diffraction (WAXD) patterns of different aerogels.

These observations indicate that the formation of the silica structure in the cellulose gel differs from that in a cellulose-free solution (regular sol–gel method). Gelation of silica in the sol–gel process is known to proceed by formation of primary silica nanoparticles, followed by their random coagulation to form an isotropic three-dimensional network.[1b] In contrast, the formation of silica nanoparticles in the cellulose gel seems to cause their deposition onto the cellulose fibrils. As a result, removal of cellulose by calcination results in the nanofibrillar silica network (Figures 2c and 3c). The fibrils appear to be around 10 nm wide, which is in agreement with the nitrogen adsorption data (Figure 4 and Table 1). The BET surface area of C2-S is 664 $m^2 g^{-1}$, and thus close to that of the pure silica aerogel, which is 767 $m^2 g^{-1}$ (Table 1).

The X-ray diffraction patterns of composite aerogels (Figure 3e) are a near-systematic superposition of those of pure cellulose and pure silica, thus indicating no interference in structure formation between the components. The crystallite sizes estimated by the Scherrer equation were 4.5 nm for cellu-

Table 1: Cellulose–silica composite aerogels with different precursor concentrations.

Sample	aq. MeOH [% v/v]	TEOS in aq. MeOH [% v/v]	ρ [g cm^{-3}]	Porosity [%]	Pore volume [cm^3 g^{-1}]	BET surface area [m^2 g^{-1}]	SiO_2 in aerogel [% w/w]	Pore diameter [nm]
S0	80	30	0.19	93	1.81	767	100	20
C0	100	0	0.14	92	1.27	356	0	19
C1	80	10	0.35	81	1.43	400	24	16
C2	80	30	0.34	83	2.24	474	39	15
C2-S	80	30	0.32	88	2.71	664	100	16
C3	80	50	0.38	82	1.47	538	52	13
C4	80	70	0.41	81	0.62	555	56	4
C5	80	90	0.45	80	0.51	652	62	3
C6	10	30	0.57	70	1.81	409	25	18
C7	30	30	0.58	71	2.43	446	36	19
C8	50	30	0.50	75	1.93	460	39	17
C9	70	30	0.45	78	2.44	514	41	20
C10	90	30	0.37	82	1.84	557	45	16

C0 = cellulose-only aerogel, C1–C10 = cellulose–silica composite aerogels, C2-S = cellulose-templated silica aerogel (after calcination), S0 = silica-only aerogel (prepared from solution without cellulose by regular sol–gel method).

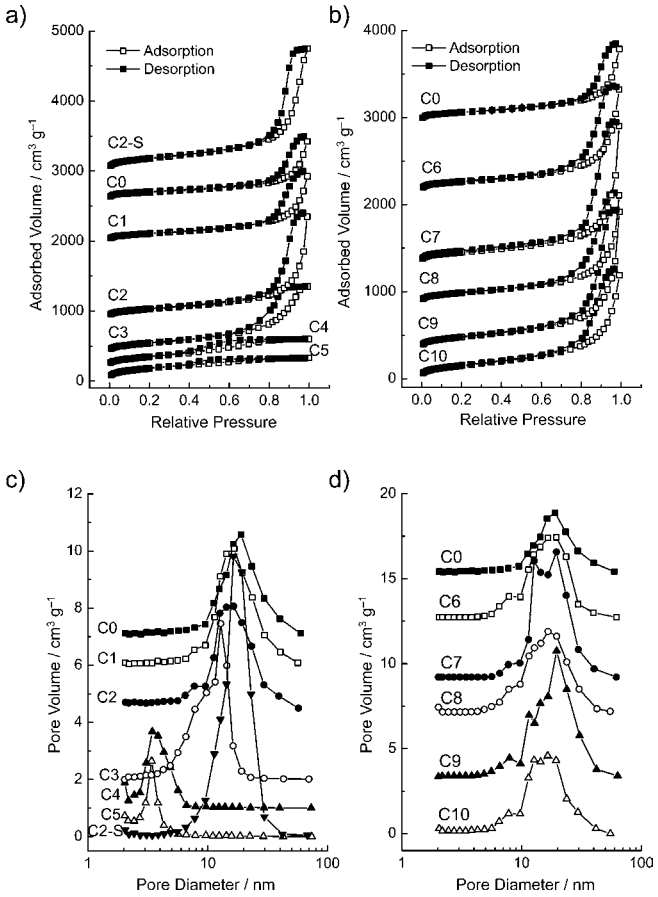

Figure 4. Nitrogen adsorption and desorption isotherms (a, b) and Barrett–Joyner–Halenda (BJH) pore-size distribution (c, d) of aerogels calculated from the desorption branch of the isotherm. Relative pressure = P/P_0.

lose and 0.9 nm for silica. These results, together with the observations made by electron microscopy, give a consistent picture, that is, the cellulose–silica composite gel/aerogel is macroscopically homogeneous, but microscopically the composites are separated to give a superposition of properties of the two components.

The nitrogen adsorption of composite aerogels changes gradually with increasing levels of silica (Figure 4a, C0–C5), however, at higher levels of silica (C4 and C5) a significant change in pore structure occurred and the isotherm leveled off at $P/P_0 > 0.6$, which translates to the loss of mesopores (Figure 4c and Table 1). This transition is understood as a result of filling the mesopore of the cellulose gel with microporous silica gel. On the other hand, the increasing amount of MeOH in MeOH/TEOS (C6–C10, Figure 4b) did not have a remarkable influence on the gel structure (Figure 4d). Still, the moderate increase in surface area by the increased MeOH concentration may be useful for controlling the properties of the composite aerogel.

The analyses presented so far of the microscopic morphology and porous structure show largely systematic changes that depend on the silica content. In terms of the macroscopic mechanical behavior, however, the composite aerogels inherited the physical integrity and flexibility of cellulose aerogel. Composite C2 was very strong and flexible (Figure 5a), with no dropping-off of silica particles on deformation. Figure 5b shows the stress–strain curves of pure cellulose and composite aerogels in tensile (in-plane) and compression (vertical-to-plane) modes. The difference is small, thus showing that the mechanical stability is provided by the cellulose network; in other words, the fragile silica component has negligible contribution to the mechanical strengths.

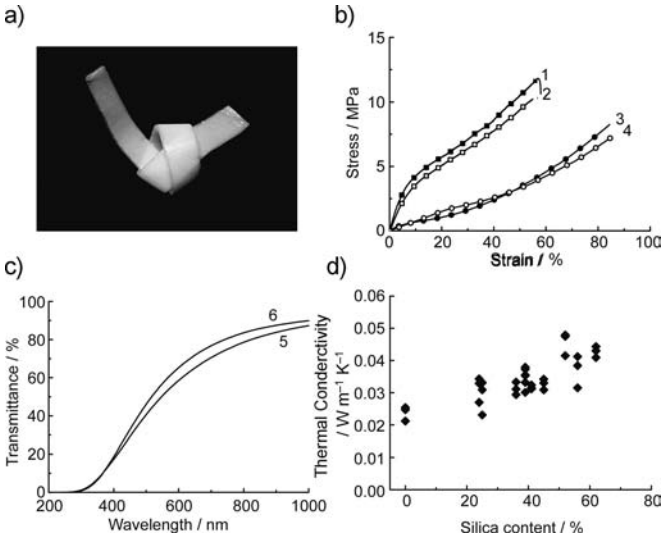

Figure 5. a) Demonstration of the flexibility of cellulose–silica composite aerogel C2. b) Stress–strain curves of C0 (curve 1: tension, curve 3: compression) and C2 (curve 2: tension, curve 4: compression). c) Optical properties of C0 (curve 5) and C2 (curve 6), both 0.35 mm thick. d) Thermal conductivity of cellulose–silica composite aerogels.

The tensile modulus and strength were determined as 72.0 MPa and 12.4 MPa for cellulose aerogel, and 48.2 MPa and 10.8 MPa for composite aerogel C2 (silica 39%; Figure 5b, curves 1 and 2). Thus the addition of silica has a slight softening effect. Under compression deformation, the modulus and collapse stress were 12.0 MPa and 0.7 MPa for cellulose, and 7.9 MPa and 1.8 MPa for the composite (Figure 5b, curves 3 and 4, respectively). The compression modulus of the composite (7.9 MPa) is more than two orders of magnitude higher than that of silica aerogel,[1a] and about 50 times higher than that of the aerogel prepared from bacterial cellulose.[6a] Notable is the large difference between tensile and compressive moduli of cellulose aerogel, that is, 72 MPa versus 12 MPa (Figure 5b). Possible causes for this behavior are 1) a difference in the mode of deformation of the three-dimensional network for stretching and compression, and 2) a possible anisotropy in the cellulose gel structure, with the cellulose fibrils aligning along the surface of the film. While such behavior has been observed for bacterial cellulose,[10] elucidation of this feature awaits further studies.

The fairly uniform nanoporosity of cellulose aerogels is manifested by their moderate light transmittance (Figure 1). Thus, the influence of the addition of silica on the optical properties of aerogels attracts attention. Figure 5c shows UV-

visible light-transmittance spectra of aerogel films. Interestingly, the transmittance of the composite with 39% silica was slightly higher than that of pure cellulose (84% vs. 79% at 800 nm), even though the density was increased from 0.14 $g\,cm^{-3}$ to 0.34 $g\,cm^{-3}$ (Table 1). A possible reason for this behavior is that filling of the void of the cellulose aerogel with silica is effective in reducing light scattering by decreasing inhomogeneity in mass distribution.

In view of the importance of thermal stability in practical applications, we examined the thermal decomposition of cellulose–silica aerogels by thermogravimetric analysis (TGA) in air and nitrogen (see Figure S1 in the Supporting Information). TGA curves of cellulose–silica aerogels showed characteristic differences in the influences of inorganic components. Thermal decomposition of cellulose is known to be promoted by the presence of metal nanoparticles (gold, platinum, and TiO_2), probably because of the catalytic effects of the metals.[8,11] In contrast, TGA of the cellulose–silica composites resulted in the decomposition of the cellulose at 300–350 °C, irrespective of the silica content, both in air and nitrogen. This observation shows that silica has a stabilizing effects on cellulose, because the DTA peak in nitrogen shifted from 318 °C to about 346 °C. The residual solid of TGA in nitrogen was black because it contained char from cellulose, while the residual solid of TGA in air was colorless white. Since the latter material was considered to be pure silica, its weight was used for calculating silica content in Table 1.

Silica aerogel is known as an excellent heat insulator.[1a] Though the presence of cellulose limits the durable temperature to below 300 °C, the composite aerogel attracts attention as heat insulator. The thermal conductivity of the composites was determined by the steady-heat-flow method with 1 mm thick polystyrene foam as standard (the thermal conductivity of this standard is 0.030 $W\,m^{-1}\,K^{-1}$; Figure 5d). In spite of the increased density of the composite from 0.14 $g\,cm^{-3}$ to about 0.6 $g\,cm^{-3}$ (Table 1), the thermal conductivity increased only moderately, from approximately 0.025 $W\,m^{-1}\,K^{-1}$ to 0.045 $W\,m^{-1}\,K^{-1}$. Since the cellulose and the composite aerogels do not soften or decompose at temperatures up to 300 °C, they can be used at much higher temperatures than common synthetic polymers. Thus the cellulose–silica composite is potentially useful as heat insulating material with high mechanical stability, together with processability to form sheets, fibers, or beads.

In summary, the regenerated cellulose gel prepared from the aqueous alkali–urea solution could serve as scaffold/template to prepare cellulose–silica composite aerogels by an in situ sol–gel process from organic silicate, and drying with supercritical CO_2. The resulting aerogels retained the mechanical strength and flexibility, large surface area, semitransparency, and low thermal conductivity of the cellulose aerogels. The ease of preparation and wide tuneability of composition/properties with this method are expected to form the basis for the development of various advanced nanoporous materials.

Received: August 12, 2011
Published online: January 24, 2012

Keywords: gels · nanocomposites · nanoparticles · polymers · thermal conductivity

[1] a) N. Hüsing, U. Schubert, *Angew. Chem.* **1998**, *110*, 22–47; *Angew. Chem. Int. Ed.* **1998**, *37*, 22–45; b) A. C. Pierre, G. M. Pajonk, *Chem. Rev.* **2002**, *102*, 4243–4265; c) A. E. Aliev, J. Y. Oh, M. E. Kozlov, A. A. Kuznetsov, S. L. Fang, A. F. Fonseca, R. Ovalle, M. D. Lima, M. H. Haque, Y. N. Gartstein, M. Zhang, A. A. Zakhidov, R. H. Baughman, *Science* **2009**, *323*, 1575–1578; d) J. L. Mohanan, I. U. Arachchige, S. L. Brock, *Science* **2005**, *307*, 397–400; e) M. A. Worsley, P. J. Pauzauskie, T. Y. Olson, J. Biener, J. H. Satcher, Jr., T. F. Baumann, *J. Am. Chem. Soc.* **2010**, *132*, 14067–14069; f) I. U. Arachchige, S. L. Brock, *J. Am. Chem. Soc.* **2006**, *128*, 7964–7971.

[2] C. A. Morris, M. L. Anderson, R. M. Stroud, C. I. Merzbacher, D. R. Rolison, *Science* **1999**, *284*, 622–624.

[3] a) N. Leventis, *Acc. Chem. Res.* **2007**, *40*, 874–884; b) N. Leventis, A. Sadekar, N. Chandrasekaran, C. Sotiriou-Leventis, *Chem. Mater.* **2010**, *22*, 2790–2803; c) M. A. B. Meador, L. A. Capadona, L. McCorkle, D. S. Papadopoulos, N. Leventis, *Chem. Mater.* **2007**, *19*, 2247–2260; d) D. J. Boday, P. Y. Keng, B. Muriithi, J. Pyun, D. A. Loy, *J. Mater. Chem.* **2010**, *20*, 6863–6865; e) H. Zou, S. Wu, J. Shen, *Chem. Rev.* **2008**, *108*, 3893–3957.

[4] D. Klemm, B. Heublein, H. P. Fink, A. Bohn, *Angew. Chem.* **2005**, *117*, 3422–3458; *Angew. Chem. Int. Ed.* **2005**, *44*, 3358–3393.

[5] a) S. J. Eichhorn, A. Dufresne, M. Aranguren, N. E. Marcovich, J. R. Capadona, S. J. Rowan, C. Weder, W. Thielemans, M. Roman, S. Renneckar, W. Gindl, S. Veigel, J. Keckes, H. Yano, K. Abe, M. Nogi, A. N. Nakagaito, A. Mangalam, J. Simonsen, A. S. Benight, A. Bismarck, L. A. Berglund, T. Peijs, *J. Mater. Sci.* **2010**, *45*, 1–33; b) J. R. Capadona, K. Shanmuganathan, D. J. Tyler, S. J. Rowan, C. Weder, *Science* **2008**, *319*, 1370–1374; c) K. Shanmuganathan, J. R. Capadona, S. J. Rowan, C. Weder, *Prog. Polym. Sci.* **2010**, *35*, 212–222; d) H. Sehaqui, M. Salajkova, Q. Zhou, L. A. Berglund, *Soft Matter* **2010**, *6*, 1824–1832.

[6] a) R. T. Olsson, M. A. Azizi Samir, G. Salazar-Alvarez, L. Belova, V. Strom, L. A. Berglund, O. Ikkala, J. Nogues, U. W. Gedde, *Nat. Nanotechnol.* **2010**, *5*, 584–588; b) M. Kettunen, R. J. Silvennoinen, N. Houbenov, A. Nykanen, J. Ruokolainen, J. Sainio, V. Pore, M. Kemell, M. Ankerfors, T. Lindstrom, M. Ritala, R. H. A. Ras, O. Ikkala, *Adv. Funct. Mater.* **2011**, *21*, 510–517.

[7] J. Cai, S. Kimura, M. Wada, S. Kuga, L. Zhang, *ChemSusChem* **2008**, *1*, 149–154.

[8] J. Cai, S. Kimura, M. Wada, S. Kuga, *Biomacromolecules* **2009**, *10*, 87–94.

[9] M. Litschauer, M.-A. Neouze, E. Haimer, U. Henniges, A. Potthast, T. Rosenau, F. Liebner, *Cellulose* **2011**, *18*, 143–149.

[10] M. Nogi, H. Yano, *Adv. Mater.* **2008**, *20*, 1849–1852.

[11] J. Zeng, S. L. Liu, J. Cai, L. Zhang, *J. Phys. Chem. C* **2010**, *114*, 7806–7811.

